

in favor of a stepwise mechanism.⁶ Although the experiments gave no positive evidence for the structure of the intermediate, it was suggested that a metallaoxetane could be involved in the reaction.

Two recent theoretical studies have been published that are relevant for the topic of this work. Houk et al.⁷ reported ab initio and DFT calculations that show that the [3 + 2] addition of SO₃ to ethylene, yielding ethylsulfite, has a *higher* barrier than the [2 + 2] addition giving the four-membered cyclic sulfone. It follows that the formally symmetry-forbidden [2 + 2] addition can become more favorable than the [3 + 2] addition. An explanation for the reversal of the activation barriers was given in terms of the strongly polarized frontier orbitals of SO₃, which has the LUMO essentially localized at sulfur and the HOMO localized at the oxygen atoms.⁷

The second important work was recently published by Rappé et al.⁸ These workers calculated the reaction energies for the addition of LReO₃ (L = Cp*, Cp, Cl, CH₃, OH, OCH₃, O⁻) to ethylene, yielding either the dioxyate via [3 + 2] addition or the oxetane via [2 + 2] addition. It was found that for L = Cp* and Cp the dioxyate is lower in energy than the oxetane, whereas the oxetane isomer becomes more stable than the dioxyate when L = Cl, CH₃, OH, OCH₃, or O⁻. This was explained with the π -donor strength of L. It was suggested that stronger π -donor ligands L favor the formation of the dioxyate over the oxetane, because in the five-membered ring only a single oxo and L compete for π -bonding with the metal.⁸ This is not a very convincing argument, because the stronger π -donor ligand, O⁻, yields the least stable dioxyate investigated in the work.⁸ Although Rappé et al.⁸ focused on the thermodynamics of the reaction, they did mention the calculated barrier for the [3 + 2] addition of CpReO₃ to ethylene (27.2 kcal/mol) and the per deuterium kinetic isotope effect (KIE) (1.09). Because both values are in very good agreement with the experimental results for the ethylene extrusion from Cp*ReO₃-C₂H₄ dioxyate reported by Gable^{6c}, the authors suggest that a [3 + 2] mechanism may be operating. However, the activation barrier and the KIE for the competitive [2 + 2] addition were not given. Also, there was no explanation why the [3 + 2] barrier for CpReO₃ addition is much higher than that for the OsO₄ addition to ethylene.

In this work, we report the calculated potential energy surfaces for the [3 + 2] and [2 + 2] addition of LReO₃ (L = O⁻, Cl, Cp) to ethylene and for the interconversion of the metallaoxetane to the dioxyates, using density functional theory (DFT) at the B3LYP⁹ level. We present the optimized transition states and equilibrium geometries of the LReO₃-C₂H₄ species, and we compare the results with the osymlation reaction. The electronic structure of the molecules is analyzed with the help of the natural bond orbital (NBO) partitioning scheme¹⁰ and the charge decomposition analysis (CDA).¹¹ The aim of this study is to understand the reason for the significantly different activation barriers and reaction energies of the addition of transition-metal oxides to ethylene.

Methods

The geometries of the molecules have been optimized using the three-parameter fit of the exchange potentials introduced by Becke (B3LYP).⁹ Relativistic small-core ECPs¹² with a valence basis set splitting (441/2111/21) were used for Re, and 6-31G(d) all-electron basis sets were employed for the other atoms.¹³ This is our standard basis set II.¹⁴ Vibrational frequencies and zero-point energy contributions (ZPE) have also been calculated at B3LYP/II. All structures reported here are either minima ($i = 0$) or transition states ($i = 1$) on the potential energy surface. The ZPE corrections are unscaled.

Improved total energies were calculated at the B3LYP level, using the same ECP and valence basis set for Re, but totally uncontracted and augmented with one set of f-type polarization functions ($\zeta = 0.869$),¹⁵ together with 6-31+G(d) basis sets for the other atoms.¹⁶ This basis set combination is denoted III+, because it is an uncontracted and augmented version of our standard basis set III.¹⁴ The calculations were carried out with the program package Gaussian 94.¹⁷

The donor-acceptor interaction in the [3 + 2] transition states have been examined using the charge-decomposition analysis (CDA).¹¹ In the CDA method, the (canonical, natural or Kohn-Sham) molecular orbitals of a complex are expressed in terms of the MOs of appropriately chosen fragments. In the present case, the Kohn-Sham orbitals of the [3 + 2] transition state for the metal oxide (MeO) addition to C₂H₄ are expressed by a linear combination of the orbitals of MeO and C₂H₄ calculated in the transition-state geometry. The orbital contributions are divided into the mixing of the occupied MOs of C₂H₄ and the unoccupied MOs of MeO (donation C₂H₄ → MeO), mixing of the unoccupied MOs of C₂H₄ and the occupied MOs of MeO (backdonation C₂H₄ ← MeO), and mixing of the occupied MOs of C₂H₄ and the occupied MOs of MeO (repulsive polarization C₂H₄ ↔ MeO). A fourth term denoted as residue term Δ gives the mixing of the unoccupied MOs of C₂H₄ and the unoccupied MOs of MeO. The Δ term should be ~ 0 if the [3 + 2] transition states can be discussed in terms of closed-shell interactions (cycloaddition between MeO and C₂H₄). Previous work has shown that this is not valid for the transition state of the formal [2 + 2] transition state of OsO₄ and ethylene.^{4a} A more detailed presentation of the method and the interpretation of the results is given in ref 11. Further examples in which the CDA method was used for the analysis of donor-acceptor complexes can be found in the literature.¹⁸ The CDA calculations have been performed using the program CDA 2.1.¹⁹

Results

There are six stationary points on the potential energy surfaces for the addition reactions of the metal oxides MeO to ethylene that are relevant for the present study. Figure 1 shows the optimized structures at B3LYP/II for the educts, transition states for [3 + 2] addition, dioxyates, transition states for [2 + 2] addition, oxetanes, and transition states for the oxetane → dioxyate rearrangements for MeO = OsO₄, ReO₄⁻, ClReO₄,

(12) Hay, P. J.; Wadt, W. R. *J. Chem. Phys.* **1985**, *82*, 299.

(13) (a) Binkley, J. S.; Pople, J. A.; Hehre, W. J. *J. Am. Chem. Soc.* **1980**, *102*, 939. (b) Hehre, W. J.; Ditchfield, R.; Pople, J. A. *J. Chem. Phys.* **1972**, *56*, 2257.

(14) Frenking, G.; Antes, I.; Böhme, M.; Dapprich, S.; Ehlers, A. W.; Jonas, V.; Neuhaus, A.; Otto, M.; Stegmann, R.; Veldkamp, A.; Vyboishchikov, S. F. In *Reviews in Computational Chemistry*; Lipkowitz, K. B., Boyd, D. B., Eds.; VCH: New York, 1996, Vol. 8, p 63.

(15) Ehlers, A. W.; Böhme, M.; Dapprich, S.; Gobbi, A.; Höllwarth, A.; Jonas, V.; Köhler, K. F.; Stegmann, R.; Veldkamp, A.; Frenking, G. *Chem. Phys. Lett.* **1993**, *208*, 111.

(16) Clark, T.; Chandrasekhar, J.; Spitznagel, G. W.; Schleyer, P. v. R. *J. Comput. Chem.* **1983**, *4*, 294.

(17) Frisch, M. J.; Trucks, G. W.; Schlegel, H. B.; Gill, P. M. W.; Johnson, B. G.; Robb, M. A.; Cheeseman, J. R.; Keith, T. A.; Petersson, G. A.; Montgomery, J. A.; Raghavachari, K.; Al-Laham, M. A.; Zakrzewski, V. G.; Ortiz, J. V.; Foresman, J. B.; Cioslowski, J.; Stefanov, B. B.; Nanayakkara, A.; Challacombe, M.; Peng, C. Y.; Ayala, P. Y.; Chen, W.; Wong, M. W.; Andres, J. L.; Replogle, E. S.; Gomberts, R.; Martin, R. L.; Fox, D. J.; Binkley, J. S.; Defrees, D. J.; Baker, I.; Stewart, J. J. P.; Head-Gordon, M.; Gonzalez, C.; Pople, J. A. *Gaussian 94*; Gaussian Inc.: Pittsburgh, PA, 1995.

(6) (a) Gable, K. P.; Phan, T. N. *J. Am. Chem. Soc.* **1994**, *116*, 833. (b) Gable, K. P.; Juliette, J. J. *J. Am. Chem. Soc.* **1995**, *117*, 955. (c) Gable, K. P.; Juliette, J. J. *J. Am. Chem. Soc.* **1996**, *118*, 2625.

(7) Haller, J.; Beno, B. R.; Houk, K. N. *J. Am. Chem. Soc.* **1998**, *120*, 6468.

(8) Pietsch, M. A.; Russo, T. V.; Murphy, R. B.; Martin, R. L.; Rappé, A. K. *Organometallics* **1998**, *17*, 2716.

(9) Becke, A. D. *J. Chem. Phys.* **1993**, *98*, 5648.

(10) Reed, A. E.; Curtiss, L. A.; Weinhold, F. *Chem. Rev.* **1988**, *88*, 899.

(11) Dapprich, S.; Frenking, G. *J. Phys. Chem.* **1995**, *99*, 9352.

and CpReO₄. In the cases of ClReO₃ and CpReO₃, we located cis and trans isomers for TS[2 + 2], oxetane, and Ts[rearr]. Table 1 gives the energies of the calculated species.

The relative energies of the stationary points change significantly at B3LYP when the large basis set III+ is used instead of II. The activation barriers become higher, and the reaction energies become more positive (less negative) at B3LYP/III+ (Table 1). The largest changes (12.3–15.3 kcal/mol) are found for the formation of the dioxylate. However, the energy ordering of the stationary points is in most (but not all) cases not affected. Nevertheless, the change in the predicted activation barriers and reaction energies does have some meaning. For example, the activation barrier OsO₄–TS[3 + 2] increases at B3LYP/III+ to 11.8 kcal/mol (13.7 kcal/mol when ZPE corrections are included). Previous DFT calculations predicted an activation energy of only 1.8 kcal/mol for the [3 + 2] addition of OsO₄ to ethylene.^{4c} Because the base-free osmylation reaction is rather sluggish,²⁰ we think that the higher activation barrier is more accurate. The calculated reaction energy for formation of OsO₄–dioxylate at B3LYP/III+ becomes –19.1 kcal/mol (–14.4 kcal/mol with ZPE corrections), which is significantly less exothermic than that predicted at B3LYP/II (–32.3 kcal/mol, –27.6 kcal/mol with ZPE corrections). The calculated barriers for the two-step mechanism B (Scheme 1) involving TS[2 + 2] (47.9 kcal/mol) and TS[rearr] (45.4 kcal/mol) at B3LYP/III+ remain much higher in energy than the barrier for the [3 + 2] addition. Because the larger basis set III+ appears to give more reliable energies, we will from now on only discuss B3LYP/III+ energies, unless it is otherwise specified.

The calculated energies for the osmylation reaction have been used to estimate the accuracy of the B3LYP/III+ results by comparing them with data obtained at the CCSD(T) level of theory. Table 1 shows that the B3LYP/III+ values for the activation barriers and reaction energies are not very different from the CCSD(T)/II results. The differences between the two levels of theory are less than 4 kcal/mol. To test the influence of the size of the basis set on the CCSD(T) results, we carried out CCSD(T) energy calculations for the [3 + 2] addition, using the much larger basis set III. Table 1 shows that the activation barrier at CCSD(T)/III+ (11.0 kcal/mol, 12.9 kcal/mol with ZPE corrections) is only slightly higher than that at CCSD(T)/II (9.6 kcal/mol, 11.5 kcal/mol with ZPE corrections). The reaction energy for formation of the dioxylate at CCSD(T)/III+ (–15.2 kcal/mol, –10.5 kcal/mol with ZPE corrections) is somewhat less exothermic than that at CCSD(T)/II (–21.2 kcal/mol, –16.5 kcal/mol with ZPE corrections). Because B3LYP/III+ mimics the CCSD(T)/III+ results even better than CCSD(T)/II, it follows that the energies predicted at the B3LYP/III+ level should be quite accurate.

The calculated reaction profile for the addition of ReO₄[–] to ethylene clearly differs from the osmylation reaction (Table 1). The dioxylate formation with perrhenate is highly endothermic (30.8 kcal/mol, 34.7 kcal/mol with ZPE corrections), whereas

the [3 + 2] addition of OsO₄ is strongly exothermic (–19.1 kcal/mol, –14.4 kcal/mol with ZPE corrections). The recent work of Rappé et al.⁸ gave a value of 33 kcal/mol for the reaction energy, in good agreement with our results. Our data confer also the prediction by Rappé that the formation of ReO₄[–]–oxetane is less endothermic than the formation of ReO₄[–]–dioxylate (Table 1). This is opposite to the OsO₄–C₂H₄ system, in which the OsO₄–dioxylate formation is clearly exothermic whereas the formation of the energetically much higher lying OsO₄–oxetane isomer is endothermic. The higher stability of ReO₄[–]–oxetane over ReO₄[–]–dioxylate is predicted only at B3LYP/III+, however. At B3LYP/II, ReO₄[–]–dioxylate is lower in energy than ReO₄[–]–oxetane (Table 1).

Although the [2 + 2] addition yielding ReO₄[–]–oxetane is thermodynamically favored over the [3 + 2] addition leading to ReO₄[–]–dioxylate, the latter reaction still has an activation barrier (44.8 kcal/mol, 46.5 kcal/mol with ZPE corrections) lower than that of the [2 + 2] addition (50.6 kcal/mol, 51.6 kcal/mol with ZPE corrections). The calculations predict that for the [3 + 2] addition to ethylene ReO₄[–] has a barrier much higher than that for OsO₄, whereas the barriers for the [2 + 2] addition steps are nearly the same (Table 1). The energy difference between TS[3 + 2] and TS[2 + 2] for the OsO₄–C₂H₄ reaction is 36.1 kcal/mol (35.5 kcal/mol with ZPE corrections) in favor of the former barrier, but it is only 5.8 kcal/mol (5.1 kcal/mol with ZPE corrections) in favor of TS[3 + 2] for the system ReO₄[–]–C₂H₄. Please note that the barrier for the rearrangement TS[rearr] is much higher (108.1 kcal/mol, 109.7 kcal/mol with ZPE) for ReO₄[–]–C₂H₄ than for OsO₄–C₂H₄ (45.4 kcal/mol, 47.4 kcal/mol with ZPE). This means that reaction course B can safely be excluded for the addition of ReO₄[–] to ethylene, although the first step has a barrier only slightly higher than that of the [3 + 2] addition.²¹ A barrier for the [3 + 2] ReO₄[–] addition to ethylene higher than that for OsO₄ is in agreement with experimental observations that the addition of osmiumtetroxide to olefins is much faster than the addition of perrhenate.⁶

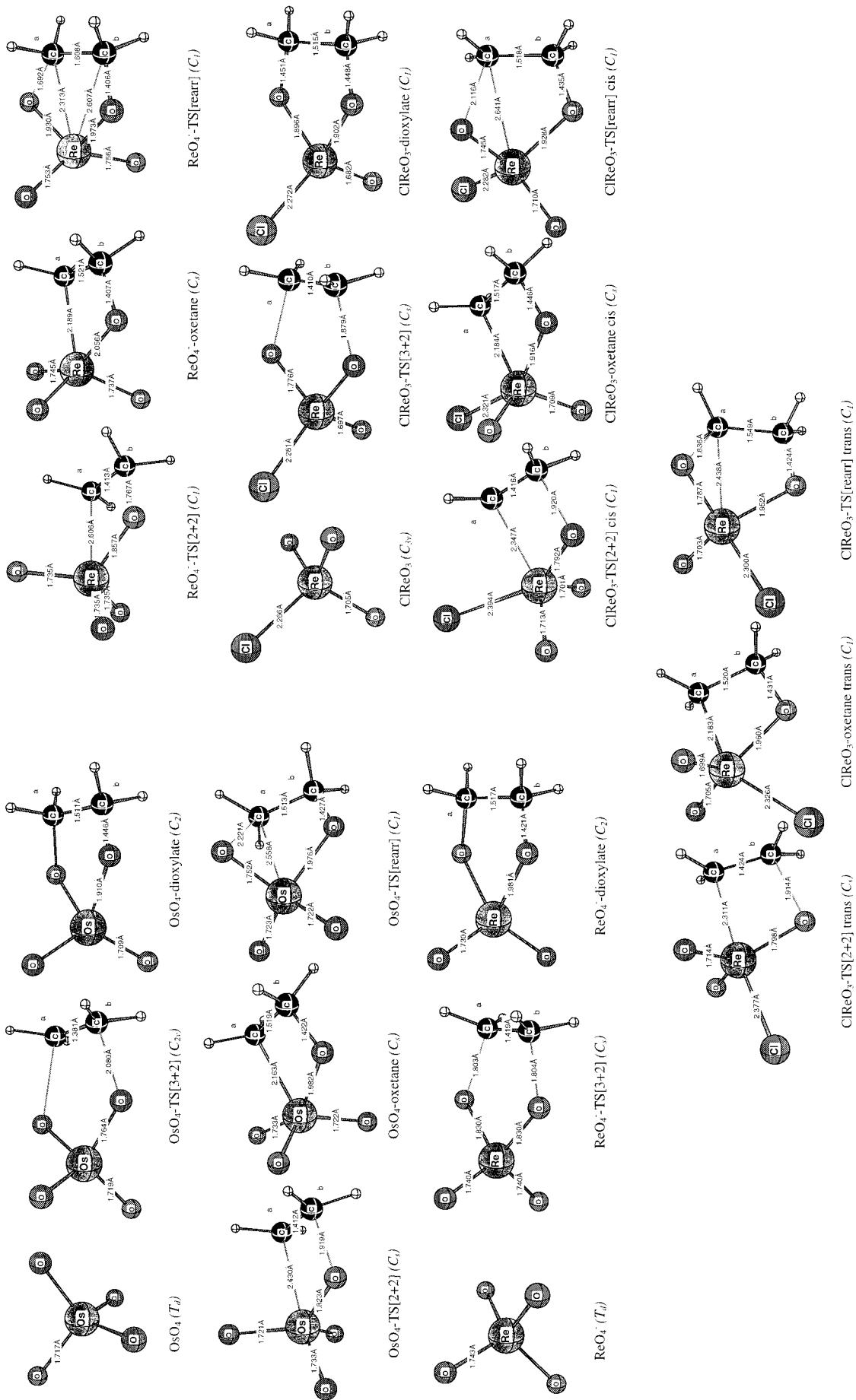
The [3 + 2] addition of ClReO₃ to ethylene is kinetically and thermodynamically less favorable than the osmylation reaction but more favorable than the ReO₄[–] addition (Table 1). The calculated barrier is 30.6 kcal/mol (32.8 kcal/mol with ZPE). The reaction is endothermic by 14.7 kcal/mol (19.3 kcal/mol with ZPE). We discuss only the energetically lowest lying cis or trans isomeric forms for the [2 + 2] addition of ClReO₃ to ethylene. The cis form has the lower barrier (34.5 kcal/mol; 36.0 kcal/mol with ZPE), which is still higher than that for TS[3 + 2]. The trans form of the ClReO₃–oxetane is lower in energy than the cis form. The formation of the former is endothermic by 9.2 kcal/mol (12.6 kcal/mol with ZPE). Because the energy barrier for interconversion of cis and trans forms is most probably lower than the activation energy for the [2 + 2] addition, it is justified to discuss the cis form of TS[2 + 2] and the trans form of the oxetane. Even if the hypothesis of a lower activation barrier for the cis–trans isomerization is not correct, it would not change the conclusion about the initial reaction step of the metal oxide addition to ethylene, because this is determined by the barrier heights of the [2 + 2] and [3 + 2]

(18) (a) Frenking, G.; Pidun, U. *J. Chem. Soc., Dalton Trans.* **1997**, 1653. (b) Pidun, U.; Frenking, G. *J. Organomet. Chem.* **1996**, 525, 269. (c) Pidun, U.; Frenking, G. *Organometallics* **1995**, 14, 5325. (d) Dapprich, S.; Frenking, G. *Organometallics* **1996**, 15, 4547. (e) Dapprich, S.; Frenking, G. *Angew. Chem.* **1995**, 107, 383; *Angew. Chem., Int. Ed. Engl.* **1995**, 34, 354. (f) Ehlers, A. W.; Dapprich, S.; Vyboishchikov, S. F.; Frenking, G. *Organometallics* **1996**, 15, 105. (g) Vyboishchikov, S. F.; Frenking, G. *Chem. Eur. J.* **1998**, 4, 1428. (h) Vyboishchikov, S. F.; Frenking, G. *Chem. Eur. J.* **1998**, 4, 1439. (i) Frenking, G.; Dapprich, S.; Köhler, K. F.; Koch, W.; Collins, J. R. *Mol. Phys.* **1996**, 89, 1245. (k) Fau, S.; Frenking, G. *Mol. Phys.*, in print.

(19) Dapprich, S.; Frenking, G. Marburg; *CDA 2.1*; 1994. The program is available via: ftp.chemie.uni-marburg.de/pub/cda.

(20) Schröder, M. *Chem. Rev.* **1980**, 80, 187.

(21) It is theoretically possible that a metallaoxetane is formed during the reaction course, because TS[2 + 2] is energetically lower than TS[3 + 2], and that the dioxylate is still produced through [3 + 2] addition, because TS[rearr] is higher than TS[3 + 2]. A scenario with relative activation energies TS[2 + 2] < TS[3 + 2] < TS[rearr] would be an alternative two-step mechanism with the oxetane as intermediate, which has previously not been considered. The calculated reaction profile for ReO₄[–] addition to ethylene shows that such a reaction path is perhaps more likely than via TS[rearr].



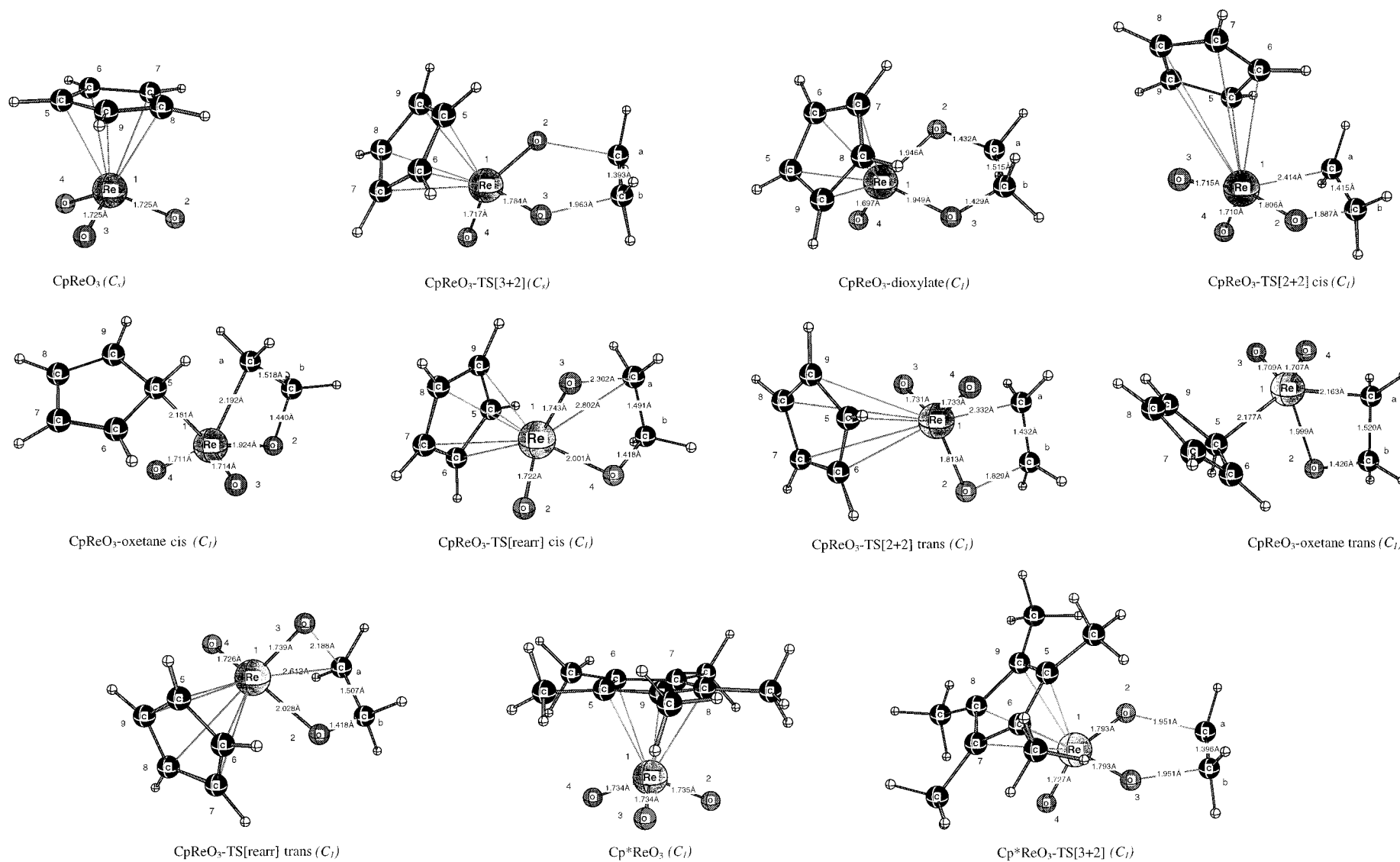


Figure 1. Optimized (B3LYP/II) geometries of the equilibrium structures and transition states. Distances are given in Å.

Table 1. Calculated Relative Energies (E_{rel}) for the Stationary Points of the [3 + 2] and [2 + 2] Additions of Metal Oxides (LMO₃) to Ethylene

LMO ₃	method	E_{rel} (kcal/mol) ^a					
		LMO ₃ + C ₂ H ₄	TS[3 + 2]	dioxylate	TS[2 + 2]	oxetane	TS[rearr]
OsO ₄	B3LYP/II ^b	0.0	5.0	-32.3	44.0	5.0	36.2
		(0.0)	(6.9)	(-27.6)	(45.3)	(8.2)	(38.4)
OsO ₄	B3LYP/III+//B3LYP/II	0.0	11.8	-19.1	47.9	12.7	45.4
		(0.0)	(13.7)	(-14.4)	(49.2)	(15.9)	(47.6)
OsO ₄	CCSD(T)/II//B3LYP/II ^b	0.0	9.6	-21.2	44.7	11.1	41.8
		(0.0)	(11.5)	(-16.5)	(46.0)	(14.3)	(44.0)
OsO ₄	CCSD(T)/III+//B3LYP/II	0.0	11.0	-15.2			
		(0.0)	(12.9)	(-10.5)			
ReO ₄ ⁻	B3LYP/II	0.0	36.0	15.5	46.2	19.1	95.4
		(0.0)	(37.7)	(19.4)	(47.2)	(21.6)	(97.0)
ReO ₄ ⁻	B3LYP/III+//B3LYP/II	0.0	44.8	30.8	50.6	27.2	108.1
		(0.0)	(46.5)	(34.7)	(51.6)	(29.7)	(109.7)
ClReO ₃	B3LYP/II	0.0	21.8	1.4	30.0; 35.2	5.9; 2.2	52.2 ^d ; 49.8
		(0.0)	(24.0)	(6.0)	(31.8; 36.8)	(9.1; 5.6)	(54.6; 52.2)
ClReO ₃	B3LYP/III+//B3LYP/II	0.0	30.6	14.7	34.5; 39.1	13.1; 9.2	61.8; 60.0
		(0.0)	(32.8)	(19.3)	(36.0; 40.6)	(16.3; 12.6)	(64.0; 62.4)
CpReO ₃	B3LYP/II	0.0 ^d	13.6	-21.0	25.4; 33.3	-2.2; -6.3	49.3 ^d ; 49.6 ^d
		(0.0)	(15.7)	(-16.1)	(27.0; 34.6)	(0.8; -3.3)	(51.2; 51.8)
CpReO ₃	B3LYP/III+//B3LYP/II	0.0	20.7	-8.7	29.9; 37.8	4.7; 0.9	58.3; 60.0
		(0.0)	(22.8)	(-3.9)	(31.6; 39.2)	(7.8; 3.8)	(60.2; 62.2)
Cp*ReO ₃	B3LYP/II	0.0	16.8		41.5 ^c ; 40.3 ^c		
		(0.0)	(18.9)				
Cp*ReO ₃	B3LYP/III+//B3LYP/II	0.0	23.0				
		(0.0)	(25.1)				

^a In cases where cis and trans isomers are found, the value for the cis isomer is given first and the value for the trans isomer is given second. ZPE(B3LYP/II)-corrected relative energies are given in parentheses. ^b Ref 4a. ^c From a geometry taken from the analogous Cp system; only internal Cp* coordinates and Re-C(Cp*) distances were optimized. ^d Instability of the restricted wave function. The unrestricted ansatz leads to an energy correction lower than 0.1 kcal/mol.

additions. The barrier for rearrangement TS[rearr] of ClReO₃ is very high (60.0 kcal/mol, 62.4 kcal/mol with ZPE). It follows that the two-step mechanism B can also be excluded for the addition of ClReO₃ to ethylene.

The central part of this work concerns the question of whether reaction path B via [2 + 2] addition is energetically possible for the addition of CpReO₃ to ethylene, because kinetic studies led to the suggestion that this path may be more favorable for Cp*ReO₃ addition to olefins than for the [3 + 2] addition.⁶ Although we model Cp* with Cp, we believe that the calculated results for the CpReO₃-C₂H₄ system are valid for Cp*ReO₃-C₂H₄ as well.

Table 1 shows that the activation barrier for the [3 + 2] addition (20.7 kcal/mol, 22.8 kcal/mol with ZPE) is higher than that for the osmylation reaction but lower than the corresponding barriers for ReO₄⁻ and ClReO₄. The formation of CpReO₃-dioxylate is exothermic by -8.7 kcal/mol (-3.9 kcal/mol with ZPE). Thus, CpReO₃ is the only LReO₃ system studied in this work which forms a dioxylate exothermically. This is in agreement with the work of Rappé, who investigated LReO₃ with L = Cp*, Cp, Cl, CH₃, OH, OCH₃, and O⁻.⁸ They calculated a reaction energy of -8 kcal/mol for the [3 + 2] addition of CpReO₄ to ethylene, which is essentially the same as our result. The [3 + 2] addition of Cp*ReO₃ to ethylene was predicted to be exothermic by -4 kcal/mol, whereas the other LReO₃ compounds have positive reaction energies.⁸ The similar values for the thermodynamics of dioxylate formation of CpReO₃ and Cp*ReO₃ support our model of using Cp instead of Cp*.

The calculated activation barrier for the [2 + 2] addition of CpReO₃ to C₂H₄ is 29.9 kcal/mol (cis form; 31.6 kcal/mol with ZPE). This means that already the first step of path B (Scheme 1) has a barrier 10 kcal/mol higher than that in path A. The formation of the CpReO₃-oxetane intermediate is slightly endothermic by 0.9 kcal/mol (trans form; 3.8 kcal/mol with

ZPE). A much higher barrier of 58.3 kcal/mol (cis form; 60.2 kcal/mol with ZPE) is predicted for the second step of path B (Table 1). The calculations clearly show that, for the addition of CpReO₃ to ethylene, the two-step mechanism via initial [2 + 2] addition has activation barriers much higher than that of the [3 + 2] cycloaddition and therefore, should *not* take place. Because of the rather large energy difference between path A and path B for CpReO₃ and because CpReO₃ should mimic the reaction profile for Cp*ReO₃ addition to ethylene quite well, we think that the reaction of olefins with Cp*ReO₃ also occurs via [3 + 2] addition.

To investigate the differences in the activation energies between Cp*ReO₃ addition and CpReO₃ addition to ethylene, we also fully optimized TS[3 + 2] for the former reaction. Figure 1 shows that the geometry of TS[3 + 2] for the addition of Cp*ReO₃ to ethylene is very similar to that for the corresponding CpReO₃ addition. Table 1 shows that the activation energy for [3 + 2] addition of Cp*ReO₃ is slightly higher (23.0 kcal/mol; 25.1 kcal/mol with inclusion of ZPE) than that for CpReO₃. The theoretically predicted activation barrier of $\Delta H^\ddagger = 25.1$ kcal/mol is in excellent agreement with the measured activation barrier of 28.0 kcal/mol for oxidation of ethylene with Cp*ReO₃ as reported by Gable and Phan.^{6a} Full optimization of Ts[2 + 2] for Cp*ReO₃ addition was not possible because of the enormous computer time. We made an estimate of the energy of the transition state by using the frozen geometries of TS[2 + 2] for cis and trans additions of CpReO₃ to C₂H₄, replacing Cp by Cp*, and optimizing the Cp* moiety. Table 1 shows the calculated energies. It becomes clear that the partially optimized cis and trans [2 + 2] transition states for Cp*ReO₃ addition are significantly higher than that for TS-[3 + 2]. Although the true transition state for [2 + 2] addition may be a bit lower in energy, it is highly unlikely that it becomes lower than that for TS[3 + 2]. The large difference between the activation barriers for the two processes and the good

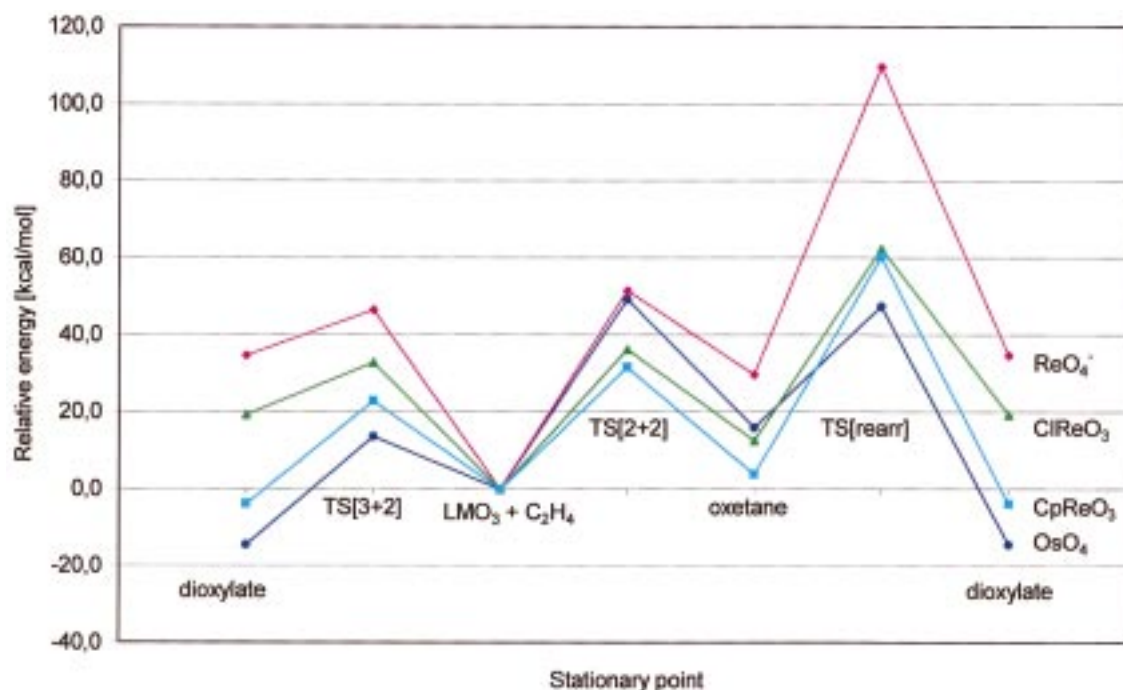


Figure 2. Schematic representation of the calculated reaction profiles for the addition of metal oxides to ethylene. Energies are taken from B3LYP/III+//B3LYP/II calculations.

Table 2. Calculated (B3LYP/II) and Experimental Re–C and C–C distances of the Structures of CpReO₃ and Cp*ReO₃ Addition to Ethylene

molecule	method	distance (Å)									
		Re–C5	Re–C6	Re–C7	Re–C8	Re–C9	C5–C6	C6–C7	C7–C8	C8–C9	C9–C5
CpReO ₃	calculated	2.474	2.488	2.481	2.481	2.488	1.426	1.418	1.431	1.418	1.426
	experimental ^a	2.341	2.377	2.429	2.429	2.377	1.434	1.400	1.505	1.400	1.434
CpReO ₃ –TS[3 + 2]	calculated	2.362	2.436	2.569	2.569	2.436	1.430	1.421	1.419	1.421	1.430
CpReO ₃ –dioxylate	calculated	2.238	2.294	2.505	2.518	2.324	1.439	1.444	1.395	1.442	1.437
	experimental ^b	2.235	2.247	2.414	2.429	2.272	1.440	1.473	1.388	1.463	1.430
CpReO ₃ –TS[2 + 2] cis	calculated	2.214	2.797	3.630	3.780	3.081	1.488	1.370	1.447	1.364	1.479
CpReO ₃ –TS[2 + 2] trans	calculated	2.300	2.558	3.301	3.591	3.101	1.448	1.401	1.430	1.376	1.462
CpReO ₃ –oxetane cis	calculated	2.181	2.932	3.836	3.911	3.090	1.495	1.357	1.462	1.353	1.502
CpReO ₃ –oxetane trans	calculated	2.177	3.006	3.823	3.786	2.935	1.498	1.356	1.461	1.362	1.484
CpReO ₃ –TS[rearr] cis	calculated	2.332	2.479	2.610	2.534	2.396	1.440	1.411	1.419	1.424	1.429
CpReO ₃ –TS[rearr] trans	calculated	2.294	2.392	2.680	2.822	2.633	1.441	1.411	1.424	1.398	1.436
Cp*ReO ₃	calculated	2.431	2.468	2.455	2.454	2.468	1.437	1.430	1.441	1.430	1.437
Cp*ReO ₃ –TS[3 + 2]	calculated	2.336	2.408	2.520	2.520	2.407	1.441	1.432	1.430	1.432	1.441

^a Ref 22. ^b Cp*ReO₃–dioxylate, ref 24.

agreement of the calculated barrier for [3 + 2] addition and the measured activation energy support our conclusion that also the Cp*ReO₃ addition to ethylene occurs via a [3 + 2] mechanism.

Figure 2 shows schematically the reaction profiles of the oxidation reactions via [2 + 2] and [3 + 2] addition for the investigated metal oxides. It becomes obvious that the [2 + 2] addition is always *kinetically* more hindered than the [3 + 2] addition, i.e., TS[2 + 2] is always higher in energy than TS[3 + 2]. This does not hold in all cases for the *thermodynamics* of the processes. The metallaoxetane forms of ReO₄[−]–C₂H₄ and ClReO₃–C₂H₄ are slightly lower in energy than the dioxylate forms, whereas the dioxylates of OsO₄–C₂H₄ and CpReO₃–C₂H₄ are more stable than the metallaoxetanes.²⁸

Important results for the addition of CpReO₃ to ethylene are given by the calculated Re–C(Cp) distances of the CpReO₃–

C₂H₄ system, which are given in Table 2. The theoretically predicted rhenium–carbon bond lengths in free CpReO₃ (2.474–2.488 Å) are slightly longer than the experimental values obtained from X-ray structure analysis (Re–C(Cp)_{av} = 2.40

(25) The energy levels of the frontier orbitals of ethylene are $\epsilon(\text{HOMO}) = -7.25$ eV and $\epsilon(\text{LUMO}) = 0.51$ eV. The energy differences to the frontier orbitals of OsO₄ (Figure 3) are $\text{HOMO}(\text{C}_2\text{H}_4) - \text{LUMO}(\text{OsO}_4) = 2.68$ eV and $\text{LUMO}(\text{C}_2\text{H}_4) - \text{HOMO}(\text{OsO}_4) = 10.57$ eV. With ReO₄[−], the energy differences become $\text{HOMO}(\text{C}_2\text{H}_4) - \text{LUMO}(\text{ReO}_4^-) = 10.79$ eV and $\text{LUMO}(\text{C}_2\text{H}_4) - \text{HOMO}(\text{ReO}_4^-) = 3.44$ eV. The energy difference $\text{LUMO}(\text{C}_2\text{H}_4) - \text{HOMO} - 1(\text{ReO}_4^-)$ is 4.28 eV.

(26) The Cp ring in CpReO₃–dioxylate could be considered η^3 -bonded ligand, because three Re–C bonds are clearly shorter than the other two Re–C bonds. However, the longer Re–C bonds in CpReO₃–dioxylate (2.505 and 2.518 Å) still have about the same interatomic distance as in free CpReO₃ (2.474–2.488 Å) and thus, indicate significant Re–C interactions.

(27) Herrmann, W. A.; Kiprof, P.; Rypdal, K.; Tremmel, J.; Blom, R.; Alberto, R.; Behm, J.; Albach, R. W.; Bock, H.; Solouki, B.; Mink, J.; Lichtenberger, D.; Gruhn, N. *J. Am. Chem. Soc.* **1991**, *113*, 6527.

(28) One referee suggested that we check the calculations for wavefunction stability with respect to spin symmetry. Few calculations were found to be UHF unstable. They are listed in Table 1. Subsequent B3LYP-(UHF) calculations gave energies which were less than 0.1 kcal/mol lower than B3LYP(RHF) energies.

(22) Kühn, F. E.; Herrmann, W. A.; Hahn, R.; Elison, M.; Blümel, J.; Herdtweck, E. *Organometallics* **1994**, *13*, 1601.

(23) Jonas, V.; Frenking, G.; Reetz, M. T. *J. Am. Chem. Soc.* **1994**, *116*, 8741.

(24) Herrmann, W. A.; März, D. W.; Herdtweck, E. *J. Organomet. Chem.* **1990**, *394*, 285. The authors do not give the Re–C distances in the paper, which can be taken from the crystallographic coordinates given in the paper.

Table 3. NBO Atomic Partial Charges and Electronic Configurations of the Metals

molecule	metal oxide			ethylene		
	6s(M)	5d(M)	q(M)	q(C _a)	q(C _b)	q(C ₂ H ₄)
ethylene				-0.44	-0.44	0.00
OsO ₄	0.32	5.43	2.22			
OsO ₄ -TS[3 + 2]	0.34	5.54	2.07	-0.29	-0.27	0.37
OsO ₄ -dioxylylate	0.38	5.67	1.89	-0.15	-0.15	0.62
OsO ₄ -TS[2 + 2]	0.35	5.52	2.08	-0.80	-0.15	0.07
OsO ₄ -oxetane	0.38	5.57	2.01	-0.66	-0.13	0.20
OsO ₄ -TS[rearr]	0.49	5.64	1.81	-0.39	-0.17	0.42
ReO ₄ ⁻	0.28	4.54	2.11			
ReO ₄ ⁻ -TS[3 + 2]	0.35	4.69	1.87	-0.35	-0.35	-0.06
ReO ₄ ⁻ -dioxylylate	0.45	4.84	1.62	-0.13	-0.13	0.47
ReO ₄ ⁻ -TS[2 + 2]	0.32	4.55	2.06	-0.85	-0.22	-0.20
ReO ₄ ⁻ -oxetane	0.34	4.65	1.95	-0.79	-0.11	-0.10
ReO ₄ ⁻ -TS[rearr]	0.38	4.79	1.74	-0.34	-0.13	0.28
ClReO ₃	0.30	4.71	1.95			
ClReO ₃ -TS[3 + 2]	0.32	4.83	1.81	-0.34	-0.34	0.30
ClReO ₃ -dioxylylate	0.34	4.99	1.63	-0.16	-0.16	0.61
ClReO ₃ -TS[2 + 2] cis	0.34	4.76	1.85	-0.76	-0.18	0.13
ClReO ₃ -TS[2 + 2] trans	0.36	4.74	1.85	-0.76	-0.13	0.18
ClReO ₃ -oxetane cis	0.34	4.77	1.84	-0.76	-0.12	0.10
ClReO ₃ -oxetane trans	0.37	4.79	1.79	-0.66	-0.12	0.19
ClReO ₃ -TS[rearr] cis	0.43	4.92	1.60	-0.40	-0.16	0.42
ClReO ₃ -TS[rearr] trans	0.46	4.93	1.55	-0.34	-0.14	0.53
CpReO ₃	0.26	4.83	1.87			
CpReO ₃ -TS[3 + 2]	0.25	4.96	1.75	-0.36	-0.36	0.22
CpReO ₃ -dioxylylate	0.27	5.18	1.50	-0.14	-0.14	0.56
CpReO ₃ -TS[2 + 2] cis	0.33	4.75	1.87	-0.77	-0.19	0.06
CpReO ₃ -TS[2 + 2] trans	0.36	4.79	1.80	-0.68	-0.19	0.16
CpReO ₃ -oxetane cis	0.33	4.76	1.87	-0.76	-0.11	0.08
CpReO ₃ -oxetane trans	0.36	4.78	1.82	-0.68	-0.11	0.14
CpReO ₃ -TS[rearr] cis	0.30	5.07	1.57	-0.39	-0.17	0.36
CpReO ₃ -TS[rearr] trans	0.39	5.03	1.52	-0.40	-0.15	0.47
CpReO ₃	0.25	4.84	1.86			
Cp*ReO ₃ -TS[3 + 2]	0.24	4.98	1.74	-0.36	-0.36	0.21

Å).²² The difference may partly be due to packing effects, which always tend to shorten bond lengths of donor-acceptor bonds.²³ More important are the changes in the Re-C distances when CpReO₃ binds to ethylene. The optimized geometry of CpReO₃-dioxylylate shows three shorter (2.238–2.324 Å) and two longer Re-C (2.505 and 2.518 Å) bonds. This means that three rhenium-carbon bonds become much shorter in CpReO₃-dioxylylate, whereas two Re-C bonds are slightly lengthened. Note that the Re-Cl distance is nearly the same in ClReO₃ and ClReO₃-dioxylylate (Figure 1). The theoretically predicted change of the Re-C distances in CpReO₃-dioxylylate are in very good agreement with the X-ray structure analysis of Cp*ReO₃-dioxylylate, which shows also a significant shortening of three Re-C bond lengths, while two Re-C distances hardly change.²⁴

More relevant for this work are the Re-C bond lengths in CpReO₃-oxetane. Figure 1 shows clearly that rhenium is η¹-bonded to the Cp ligand in the compound, which has one short (2.177 Å) and four long (2.935–3.823 Å) Re-C distances in the energetically lower lying trans form. The cis form of CpReO₃-oxetane is also η¹-bonded. Thus, the Cp ligand shows a significantly different binding behavior with rhenium when ethylene is bonded in a [2 + 2] or [3 + 2] fashion.

Discussion

To find an explanation for the large differences in the thermodynamic and kinetic results for addition of the metal oxides to ethylene, we analyzed the electronic structure of the stationary points on the potential energy surfaces. Table 3 shows the partial charges given by the NBO method. Table 4 gives the results of the charge decomposition analysis for the [3 + 2] transition states.

Because the addition of OsO₄ to ethylene is an oxidation reaction, it can be expected that the C₂H₄ moiety of the OsO₄⁻-C₂H₄ species carries a positive partial charge. Table 3 shows that the OsO₄-dioxylylate has a positive charge $q(\text{C}_2\text{H}_4) = +0.62$. About one-half of the charge transfer has already taken place at the transition state OsO₄-TS[3 + 2], which has $q(\text{C}_2\text{H}_4) = 0.37$. The charge transfer from ethylene to OsO₄ in the intermediate OsO₄-oxetane is only +0.20e (Table 3).

The results of the CDA for the interaction between OsO₄ and C₂H₄ also show that the dominant electronic flow is from ethylene to OsO₄. The amount of C₂H₄ → OsO₄ donation in OsO₄-TS[3 + 2] (0.179e) is clearly higher than the C₂H₄ ← OsO₄ backdonation (0.136e). The difference between the C₂H₄ → OsO₄ donation and C₂H₄ ← OsO₄ backdonation (0.043e) is much less, however, than the charge transfer given by the NBO method (0.37e). It means that the mixing of the occupied orbitals as given by the repulsive polarization term is largely responsible for the charge reorganization.

Figure 3 shows the frontier orbitals of the metal oxides. OsO₄ has a triply degenerate (*t*₁) HOMO and a doubly degenerate (*e*) LUMO. Both frontier orbitals are mainly p(π) orbitals at oxygen. HOMO and LUMO of OsO₄ have the right symmetry to interact with the π^* LUMO and π HOMO of ethylene in a [3 + 2] fashion, respectively, but not in a [2 + 2] way. The small value for the Δ term (0.005) of the CDA partitioning of OsO₄-TS[3 + 2] indicates that it is justified to consider the reaction step as [3 + 2] cycloaddition. A previous CDA examination of the formal [2 + 2] transition state showed that the Δ term is significantly different from zero.^{4a} Further analysis of the CDA terms shows that the HOMO(C₂H₄) → LUMO(OsO₄) donation and LUMO(C₂H₄) ← HOMO(OsO₄) backdonation are the dominant orbital contributions to the total donation and backdonation.

The [3 + 2] addition of ReO₄⁻ to ethylene has a barrier much higher than that for the OsO₄ addition. Table 3 shows that the product molecule ReO₄⁻-dioxylylate has a partial charge at the C₂H₄ moiety (+0.47e) lower than that of the OsO₄-dioxylylate. This is reasonable, because ReO₄⁻ is already negatively charged. More important is the charge distribution in the transition state ReO₄⁻-TS[3 + 2], which has a *negative* partial charge at the ethylene unit! This means that there is initially a “wrong” electron flow from the metal oxide to ethylene when ReO₄⁻ approaches C₂H₄. Although the transition state ReO₄⁻-TS[3 + 2] occurs much later on the reaction coordinate than OsO₄-TS[3 + 2], which is revealed by the longer C-C and shorter O-C distances in the former transition state (Figure 1), there is still a small negative charge of $q(\text{C}_2\text{H}_4) = -0.06$ in ReO₄⁻-TS[3 + 2] (Table 3). The importance of the repulsive interactions in ReO₄⁻-TS[3 + 2] is revealed by the CDA results (Table 4). There is a repulsive polarization substantially larger (-1.636e) than that in OsO₄-TS[3 + 2] (-0.290e). Another difference between the two [3 + 2] transition states is the relative size of donation and backdonation. The amount of C₂H₄ ← MeO backdonation *b* in ReO₄⁻-TS[3 + 2] is *higher* than the C₂H₄ → MeO donation *d*. The *d/b* ratio in ReO₄⁻-TS[3 + 2] is only 0.69, whereas *d/b* = 1.32 in OsO₄-TS[3 + 2]. This can be explained with the different energy levels of the frontier orbitals in OsO₄ and ReO₄⁻. Table 5 shows that the negatively charged ReO₄⁻ has much higher lying frontier orbitals than OsO₄, which makes the HOMO(ReO₄⁻)-LUMO(C₂H₄) interaction energetically more favorable than the LUMO(ReO₄⁻)-HOMO(C₂H₄) interaction. Interestingly, the CDA shows that the main contribution arises from the donation of HOMO-1(ReO₄⁻) to the LUMO(C₂H₄).²⁵ The HOMO-1 of ReO₄⁻ has *t*₂ symmetry

Table 4. CDA Results (B3LYP/II) for the [3 + 2] Transition States of the C₂H₄ Addition to Metal Oxides (LMO₃)

LMO ₃	<i>d</i> (donation) C ₂ H ₄ → LMO ₃	<i>b</i> (backdonation) C ₂ H ₄ ← LMO ₃	<i>d/b</i>	<i>r</i> (repulsive polarization) C ₂ H ₄ ↔ LMO ₃	Δ
OsO ₄	0.179 (0.228) ^a	0.136 (0.113) ^b	1.32	-0.290	0.005
ReO ₄ ⁻	0.191 (0.123) ^c	0.275 (0.093) ^d	0.69	-1.636	0.057
ClReO ₃	0.214 (0.233) ^e	0.228 (0.135) ^f	0.94	-0.590	0.005
CpReO ₃	0.207 (0.194) ^g	0.216 (0.106) ^h	0.96	-0.507	0.000

^a The most important contributions are given in parentheses. HOMO → LUMO. ^b LUMO ← HOMO. ^c HOMO → LUMO. ^d LUMO ← HOMO-1. ^e HOMO → LUMO. ^f LUMO ← HOMO. ^g HOMO → LUMO. ^h LUMO ← HOMO-3.

(Figure 3). However, the main reason for the large barrier of the ReO₄⁻ [3 + 2] addition to C₂H₄ is clearly the repulsion between the negatively charged metal oxide and the π-electron density of ethylene.

The calculated [2 + 2] transition states of OsO₄ and ReO₄⁻ have nearly identical C–C distances of the ethylene ligand (Figure 1), which confers with the similar activation barriers for the two processes (Table 1). Note, however, that the oxygen–carbon distance of ReO₄⁻-TS[2 + 2] (1.767 Å) is significantly shorter than that in OsO₄-TS[2 + 2] (1.919 Å), whereas the metal–carbon distance of the former is clearly longer than that in the latter TS. The calculated geometries indicate a pathway for the [2 + 2] addition of ReO₄⁻ to ethylene which is more asynchronous than that for OsO₄. The calculated charge distribution shows (Table 3) that ReO₄⁻-TS[2 + 2] and OsO₄-TS[2 + 2] have a large zwitterionic character, with the negative end at C_a and the positive end at the metal. This could be a hint towards stabilization of the [2 + 2] transition states. Olefins with push–pull substituents at the carbon atoms might lead to a kinetically favored oxetane formation. We will investigate this possibility in a future theoretical study. Note that the ethylene moiety in the intermediate ReO₄⁻-oxetane carries a small negative charge, which is even higher in ReO₄⁻-TS[2 + 2] (Table 3).

The transition state for rearrangement TS[rearr] of ReO₄⁻-C₂H₄ is much higher in energy than the [2 + 2] transition state. Figure 1 shows that the C–C distance of ReO₄⁻-TS[rearr] (1.608 Å) is much longer than that in OsO₄-TS[rearr] (1.513 Å), and it is also much longer than the energy minima to which the TS belongs, i.e., ReO₄⁻-oxetane (1.521 Å) and ReO₄⁻-dioxylylate (1.517 Å).

The energy barrier for the [3 + 2] addition of ClReO₃-C₂H₄ is intermediate between the barriers for the systems OsO₄-C₂H₄ and ReO₄⁻-C₂H₄ (Table 1). The optimized structure for ClReO₃-TS[3 + 2] shows that the calculated C–C and O–C distances are also intermediate between those for OsO₄-TS[3 + 2] and ReO₄⁻-TS[3 + 2] (Figure 1). There is a charge transfer of 0.61*e* from C₂H₄ to ClReO₃ in ClReO₃-dioxylylate (Table 3). Half of the amount (0.30*e*) is already transferred in ClReO₃-TS[3 + 2]. The CDA results (Table 4) show that C₂H₄ → ClReO₃ donation (0.214*e*) and C₂H₄ ← ClReO₃ backdonation (0.228*e*) have similar size. The *d/b* ratio of 0.94 is also intermediate between values for OsO₄-TS[3 + 2] and ReO₄⁻-TS[3 + 2]. Table 5 shows that the energy levels ε_{HOMO} and ε_{LUMO} in ClReO₃ are raised relative to those in OsO₄. The energy rise is rather small, however, and cannot be the main reason for the significantly higher activation barrier. Note that the shape of the frontier orbitals and the participation of the oxygen atoms are different between ClReO₃ and OsO₄, because the molecules have different symmetry and the number of oxygen atoms is different. For example, the HOMO of ClReO₃ is distributed exclusively over the p(π) orbitals of the three oxygens, whereas four oxygens are involved in the HOMO of OsO₄ and ReO₄⁻. This shows that a simple frontier orbital consideration is not sufficient to explain the changes in the [3 + 2] activation

energies. The results demonstrate, however, that the energy level and the distribution of the frontier orbitals of the metal oxides have a strong influence on the [3 + 2] energy barrier.

The CDA results reveal another aspect which might be important for the barriers of the [3 + 2] reaction. Table 4 shows that the repulsive interaction term C₂H₄ ↔ ClReO₃ (-0.590*e*) is clearly larger than C₂H₄ ↔ OsO₄. The negative partial charge at oxygen is higher in ClReO₃ than in OsO₄ (Table 3). This means that the initial charge repulsion between the oxygen atoms and the π-charge of ethylene for the approach of ClReO₃ is higher than that for OsO₄. This is in agreement with the CDA result.

The transition state ClReO₃-TS[2 + 2] is lower in energy than ReO₄⁻-TS[2 + 2] and OsO₄-TS[2 + 2] (Table 1). Figure 1 shows that the C–C and O–C distances of ClReO₃-TS[2 + 2] are similar to OsO₄-TS[2 + 2], but the metal–C_a distance of the former TS is clearly shorter. This could be the reason for the lower energy of ClReO₃-TS[2 + 2], because there is charge attraction between positively charged Re and negatively charged C_a (Table 3). Note that there is little correlation between the reaction energies and the activation barriers for the [2 + 2] addition reaction of the metal oxides to ethylene.

The calculated structures of the CpReO₃-C₂H₄ species indicate the special nature of the Cp ligand, which is revealed by the theoretically predicted Re–C distances (Table 2). In CpReO₃, rhenium is η⁵-bonded to the Cp ligands with Re–C distances between 2.474 and 2.488 Å. Rhenium has the formal oxidation state VII, i.e., the seven valence electrons all form chemical bonds with the ligands. There are three Re=O double bonds in CpReO₃ and one Re–Cp single bond, which becomes enhanced by Cp → Re donation from the π-electrons of the aromatic ring. The number of the rhenium–oxygen bonds in the [3 + 2] addition product CpReO₃-dioxylylate is one double and two single bonds. The formal oxidation state in LReO₃-dioxylylate is V, which means that two valence electrons at Re are not engaged in binding interactions. However, unlike for L = Cl and O⁻, the ligand L = Cp can activate additional atoms for L–Re bonding. Three Re–C bonds become significantly shorter in CpReO₃-dioxylylate compared with free CpReO₃.²⁶ Although the short Re–C distances in CpReO₃-dioxylylate (2.238–2.324 Å) are still longer than those in H₃C–ReO₃ (2.06 Å),²⁷ it becomes obvious that the Re–carbon bonding interactions become enhanced in CpReO₃-dioxylylate. The enhanced binding of the Cp ligand is *not* possible for Cl in ClReO₃-dioxylylate. Figure 1 shows that the Re–Cl distance is even slightly longer in ClReO₃-dioxylylate than in free ClReO₃. Table 2 shows that three Re–carbon distances are already shortened in CpReO₃-TS[3 + 2], and two bonds become longer. The unique property of the Cp ligand to adopt to different bonding situations seems to be the main reason for the relatively low activation barrier and exothermicity of the [3 + 2] addition of CpReO₃ to ethylene. Table 5 shows that the energy levels of the HOMO and the LUMO of CpReO₃ are raised with respect to those of ClReO₃. The CDA results given in Table 4 show that the *d/b* ratios of ClReO₃ and CpReO₃ are nearly the same.

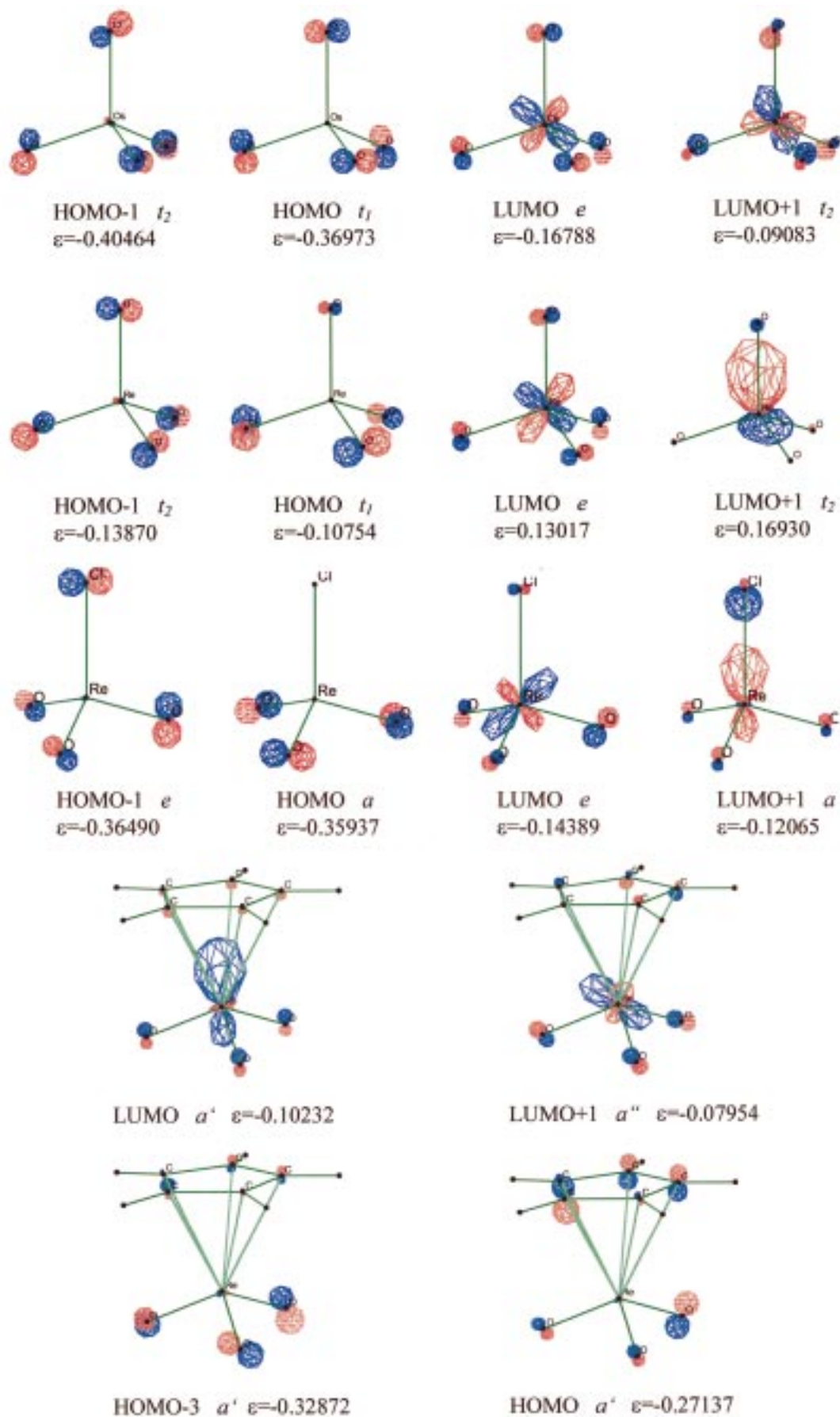


Figure 3. Plot of the frontier orbitals of the metal oxides.

Table 5. Calculated (B3LYP/III+/B3LYP/II) Activation Barriers (ΔE^\ddagger) for the [3 + 2] Addition of Metal Oxides (LMO₃) in Ethylene^a

LMO ₃	ΔE^\ddagger (kcal/mol)	<i>d/b</i>	ϵ_{HOMO}	ϵ_{LUMO}
OsO ₄	6.9	1.32	0.0	0.0
ReO ₄ ⁻	37.7	0.69	6.27 ^b	8.11
ClReO ₃	24.0	0.94	0.27	0.65
CpReO ₃	15.7	0.96	1.11 ^c	1.80

^a Ratio of donation *d* and backdonation *b* given by the CDA method; energy levels [eV] of the dominant frontier orbitals relative to OsO₄.

Both data do not readily explain why the latter metal oxide has a lower barrier for the [3 + 2] addition.

The Cp ligand also has a significant influence on the reaction course of the [2 + 2] addition of CpReO₃ to ethylene, which has the lowest activation barrier of all metal oxides that were investigated in this work. As noted above, the Cp ligand is bonded in an η^1 fashion in the CpReO₃-oxetane intermediate (Figure 1 and Table 2). The change from η^5 in free CpReO₃ to η^1 in CpReO₃-oxetane, which both have the formal oxidation state VII for rhenium, could be due to steric effects. In CpReO₃-oxetane, the rhenium atom is five-coordinate, whereas it is four-coordinate in free CpReO₃. The Cp ligand in CpReO₃-oxetane is in a pseudoaxial position, and the pseudoequatorial positions are occupied by three oxygens in the trans isomer and two oxygens and a carbon in the cis isomer (Figure 1). There are also electronic effects which favor Re-Cp(η^1) bonding. The π -component of the Re-Cp η^5 -bonding comes from electron donation from the Cp ligand into the empty d_{yz} and d_{xz} orbitals, when the *z*-axis is taken from Re to the midpoint of the Cp ligand. Then, the *xy* plane becomes the equatorial plane in CpReO₃-oxetane. There will be stronger π -bonding between Re and the terminal oxygens atoms, which becomes obvious by the shortening of the Re=O bond lengths in CpReO₃-oxetane (Figure 1). Because the Re=O π -bonding involves the d_{yz} and d_{xz} orbitals of Re, the Cp-Re π -bonding becomes less efficient.

It is puzzling at first sight that the cis isomer of CpReO₃-oxetane is higher in energy than the trans isomer, while the corresponding transition states CpReO₃-TS[2 + 2] exhibit the opposite order (Table 1). CpReO₃-TS[2 + 2]_{cis} is significantly lower (29.9 kcal/mol) than CpReO₃-TS[2 + 2]_{trans} (37.8 kcal/mol). We think that the Cp ligand has a destabilizing effect on the trans Re-C bond, because two σ -donor bonds are trans to each other. There is no σ -bond trans to Re-Cp in CpReO₃-TS[2 + 2]_{cis}. Therefore, CpReO₃-TS[2 + 2]_{trans} is higher in energy than CpReO₃-TS[2 + 2]_{cis}. The reason why the cis form of the intermediate CpReO₃-oxetane is less stable than the trans form can be explained with the same reasoning. The C(Cp)-Re σ -bond is trans to the Re-Ca σ -bond in the trans isomer and trans to the Re-O2 σ -bond in the cis isomer. Because the latter σ -bond is stronger, the unfavorable trans interactions cause CpReO₃-oxetane_{cis} to become higher in energy than CpReO₃-oxetane_{trans}.

The transition states for rearrangement are very high in energy for all metal oxides. TS[rearr] is even the highest lying transition state for LReO₃ (Table 1 and Figure 2). The large energy barrier suggests that the rearrangement is a symmetry-forbidden process. We checked the electronic structure of the oxetane intermediates, but it was not possible to specify a particular orbital that might be responsible for the large activation energy.

A final matter of discussion concerns the results of the kinetics of alkene extrusion from rhenium diolates, which have been interpreted in favor of a two-step mechanism involving metallaoxetane intermediates.⁶ The theoretical results presented by

Rappé et al.⁸ and in our work leave little doubt that the reaction takes place via a concerted [3 + 2] addition. The same situation exists for the osmylation reaction, in which kinetic studies suggested [2 + 2] addition followed by rearrangement as the reaction mechanism.² Quantum calculations clearly showed that the [3 + 2] cycloaddition is operative in the reaction.⁴ We think that a thorough analysis of the kinetic data is necessary to make the results of the kinetic measurements understandable. The question is not anymore if the reaction takes place via [3 + 2] or [2 + 2] addition. The question is why measurements of [3 + 2] additions of metal oxides to olefins give data which are not in agreement with the mechanism of the reaction.

Summary

The results of this work can be summarized as follows:

(1) The metal oxides LReO₃ (L = O⁻, Cl, Cp) have activation barriers for the [3 + 2] addition to ethylene that are significantly higher than that for OsO₄. The order for the activation energies is OsO₄ < CpReO₄ < ClReO₃ < ReO₄⁻.

(2) The activation energies for the [2 + 2] addition yielding metallaoxetanes remain in all cases higher than the barriers for the [3 + 2] reaction, but the differences between the barrier heights is much less for LReO₃ than for OsO₄. CpReO₃ and ClReO₃ have barriers for [2 + 2] addition to ethylene that are lower than that for OsO₄, whereas ReO₄⁻ has a slightly higher activation energy.

(3) The activation energies for rearrangement of the oxetane intermediate to the dioxylate is very high for LReO₃, which rules out the suggested two-step mechanism for alkene extrusion from Re(V)dioxylates.

(4) It seems possible that the addition of metal oxides LReO₃ to (1,2)pushpull-substituted olefins yields metallaoxetanes rather than dioxylates, because the carbon atoms of the metallaoxetanes have a zwitterionic character in the [2 + 2] transition state and in the product.

(5) The activation barrier for the [3 + 2] addition can be related to the frontier orbitals of the reactants, whereas the [2 + 2] addition is not a cycloaddition but rather a nucleophilic attack of the oxygen toward one carbon atom of the olefin.

(6) The Cp ligand shows unique properties as "stereoelectronic mediator" by adopting different bonding modes with the metal in CpReO₃-C₂H₄ isomers. This leads to energies for the activation barriers and reaction products which are not obvious when free CpReO₃ becomes analyzed.

Note Added in Proof: An example where the [2 + 2] addition of a transition metal oxide across a C=C double bond has a lower activation energy than the [3 + 2] addition has now been found for (R₃PN)ReO₃ + ketene: Schlecht, S.; Deubel, D. V.; Dehnicke, K.; Frenking, G. *Angew. Chem.* Submitted for publication.

Acknowledgment. We thank the Deutsche Forschungsgemeinschaft (SFB 260-D19 and Graduiertenkolleg Metallorganische Chemie) and the Fonds der Chemischen Industrie for financial support. Excellent service was provided by the computer centers HRZ Marburg, HLRZ Darmstadt, HLRS Stuttgart.